J. theor. Biol. (1983) **101**, 415–440

A Mathematical Model of the Effects of CO_2 on Stomatal Dynamics

S. K. UPADHYAYA†, R. H. RAND AND J. R. COOKE

Departments of Agricultural Engineering and Theoretical and Applied Mechanics, Cornell University, Ithaca, New York 14853, *U.S.A.*

(*Received* 2 *June* 1982, *and in revised form* 18 *November* 1982)

We extend a previous model of stomatal dynamics (Delwiche & Cooke 1977) which accounted for hydraulic feedback effects but which omitted CO_2 feedback effects. The present work includes both feedback loops in a model featuring the CO_2 chemistry of the guard cell. The model consists of three first order non-linear differential equations which are treated by numerical integration.

Introduction

Stomatal pores are microscopic openings on the leaf surface that permit the gas exchange of CO_2 and water vapor between the leaf interior and the environment. CO_2 is used by the plant in photosynthesis. When the stomatal pore is open, however, not only does CO_2 enter the leaf, but water vapor diffuses out of the leaf into the atmosphere. Water loss is undesirable, especially in times of drought. Stomates therefore have the dual task of permitting sufficient entry of CO_2 while avoiding excessive water loss.

The stomatal pore is bounded by two specialized guard cells which act as a valve in regulating pore size (Cooke *et al.*, 1976); see Fig. 1. In addition to transient responses, stomatal apertures have been observed to oscillate, even under constant environmental conditions. Experiments have revealed two oscillations: one having a 10–50 minute period associated with a hydraulic feedback loop, and another with a 2–5 minute period associated with a CO_2 feedback loop (Barrs, 1971).

Delwiche & Cooke (1977) modelled the hydropassive aspects of stomatal dynamics, but did not include the CO_2 loop. Rand *et al.* (1980) analyzed that model and showed that it exhibits a steady state oscillation for a certain

† Present address: Department of Agricultural Engineering, University of Delaware, Newark, Delaware 19711, U.S.A.

0022-5193/83/070415 + 26 $03.00/0

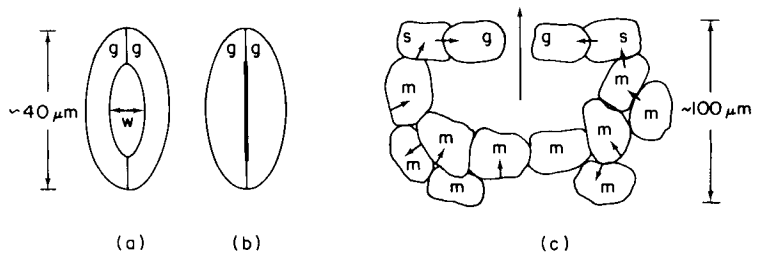

FIG. 1. The stomatal apparatus. View looking onto the leaf surface, (a) pore open, (b) pore closed. (c) Cross-sectional view with arrows representing various water fluxes (see text); g = guard cell; s = subsidiary cell; m = mesophyll cell.

range of parameter values, Fig. 2. The objective of the present study is to extend this previous work by including the effects of the CO_2 feedback loop.

In addition to both CO_2 and hydropassive loops, the current model could also include a hydroactive feedback loop. The hydroactive loop could be modeled by requiring the H^+ pump capacity or the PEP carboxylation velocity in the guard cell to be dependent upon the water potential in the mesophyll cells. This models the hypothesis (Raschke, 1979) that abscisic acid is produced in the mesophyll under water stress, and upon arriving at the guard cells, causes solute loss.

Numerical integration of the differential equations of our model reveals that the system exhibits a limit cycle in three dimensional state space. The resulting oscillation is shown to possess (1) a hydraulically-based oscillation with a period of about 20 minutes and (2) a CO_2-based oscillation with a period of about 2 minutes. The CO_2-based oscillation is superimposed on

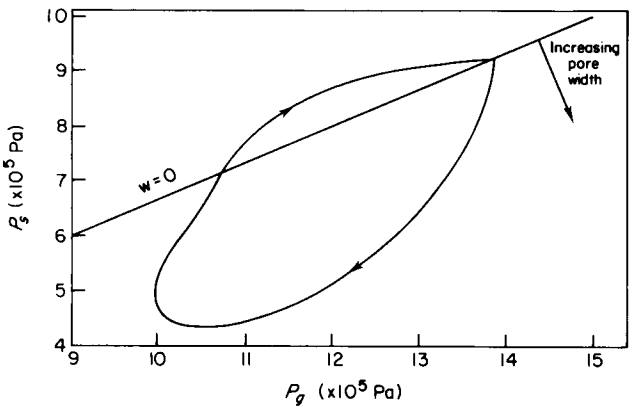

FIG. 2. Limit cycle oscillation in the P_g, P_s plane exhibited by the model involving only hydropassive feedback loop (Delwiche & Cooke, 1977). Note that the stomatal pore width $w = 0$ for all pressures P_g, P_s lying above the straight line.

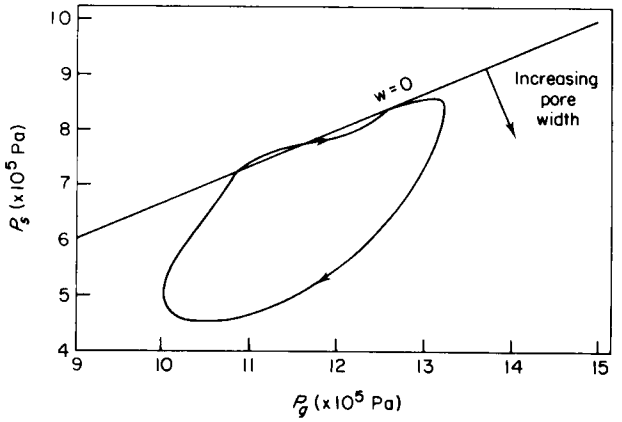

FIG. 3. Limit cycle oscillation projected onto the P_g, P_s plane exhibited by the model described in this paper. Model includes both hydropassive and CO_2 feedback loops.

the water-based oscillation (Figs 2 and 3). Note that the CO_2 oscillation occurs only when the stomatal pore is nearly closed. We will present extensive parameter studies later in this paper.

Review of Literature

The remarkable behavior of stomates has interested plant physiologists for well over a century, and the number of investigations reported in the literature is vast. Two reviews by Raschke (1975, 1979) and another by Hsiao (1976) cover the literature on all aspects of stomatal action. Cowan (1977) has reviewed the literature on stomatal behavior and the environment and has included mathematical studies in his treatment of the subject. Upadhyaya, Rand & Cooke (1980*b*), referred to as URC in the text, have provided an extensive review of various aspects of stomatal movements. The following literature review is an abbreviated summary of that given in URC.

The stomatal pore in many plants is formed by an opening between two kidney shaped guard cells. This structure is called an elliptical stomate. Another type of stomate normally found in grasses is formed by an opening between two "dumbbell-shaped" guard cells and is referred to as graminaceous (Meidner & Mansfield, 1968). Stomatal movements occur due to changes in the turgor pressures of these guard cells and the neighboring subsidiary cells. The change occurs mainly in the pore width, the pore length remaining relatively constant. Cooke *et al.* (1976, 1977) have made a linear and nonlinear finite element analysis of the guard cell mechanics.

Their results show that the pore width is linearly related to the guard cell pressure and subsidiary cell pressure when the stomate is open. Changes in the turgor of guard cell and subsidiary cells are caused by several environmental factors and the pore width can exhibit self-induced (or endogenous) oscillations even in a constant environment.

STOMATAL MOVEMENTS

Stomatal movements are controlled by three feedback mechanisms: (i) hydropassive, (ii) hydroactive and (iii) CO_2 based feedback control.

Hydropassive movements

Changes in the water potential in the leaf system produce two opposing effects on stomates. Water potential in the guard cell follows the water potential in the vascular bundle. Thus a reduction in the water potential in the conduit tends to close the stomates by decreasing the water potential of the guard cell. The second effect is due to pressure changes in the epidermis (subsidiary cells). A decrease in the water potential of these cells tends to open the stomates. The net opening of the stomate is a result of these opposing motions. This is termed hydropassive movement of stomates. Here the water potential changes simply as a direct response to water stress but solute contents do not change.

Hydroactive movements

In contrast with the above, hydroactive feedback brings about a change in the solute content of the guard cells. The hydroactive closure of stomates is brought about by a plant hormone called abscisic acid (ABA) (Raschke, 1975). The role of ABA in bringing about stomatal closure has been confirmed by many researchers. Raschke has found that open stomates of *Xantium strumarium L.* closed only when carbon dioxide and ABA were present simultaneously. Changes in stomatal response to ABA is enhanced by CO_2. This follows saturation kinetics. The simultaneous requirement of CO_2 and ABA for stomatal closure leads to the inference that ABA inhibits the expulsion of H^+ from the guard cells and acidifies the cytoplasm. The CO_2 supply has been found to enhance hydroactive closing. Raschke has proposed the following mechanism:

$$CO_2 \rightarrow \text{Malic acid } (H_2A) \rightarrow H^+ + HA^- + A^{2-}.$$

ABA inhibits active expulsion of H^+. H^+ accumulation acidifies the guard cells. Thus CO_2 is needed for stomatal closure. Endogenous CO_2 due to respiration may be sufficient in some cases.

CO_2 based movements

Stomata of plants respond to CO_2 concentration. Scarth put forward a theory which postulated conversion of starch to sugar during stomatal opening (Meidner & Mansfield, 1968). Beginning in 1968, plant physiologists have become aware that stomatal regulation by CO_2 is an active transport mechanism involving the transport of K^+ ions. Stomatal movements associated with light, CO_2, ABA or night movements have associated K^+ fluxes. Stomatal width and mean potassium content were found to be linearly related. Although there is a shuttle of K^+ and Cl^- ions, Cl^- can only partially account for the accompanying anion. The extent of the charge balance provided by Cl^- varies from 5 to 100 percent, depending on the species. It is likely that malates form the balancing anion (Raschke, 1975). The subsidiary cells are most likely the source of K^+ and also act as a reservoir for Cl^-.

Stomatal response to CO_2 is essentially the same in light and darkness. Therefore, the mechanism is probably the same in both cases. High stomatal action at low CO_2 concentration rules out stomatal action based on carbonic acid. The CO_2 sensor is located in the guard cells and is probably very close to the intercellular air space. This suggests that continuous malic acid metabolism may serve as a sensing system for CO_2 in the guard cells.

Thus stomatal opening has the following associated processes:

(1) Uptake of K^+ into the guard cell vacuole.
(2) Expulsion of H^+ from the guard cells.
(3) Production of organic acid, particularly malic acid.
(4) Disappearance of starch.
(5) Uptake of Cl^- into the vacuole.

Levitt (1974) put forward a theory that incorporated the positive points of Scarth's theory and the active K^+ transport theory. Although this theory attempts to explain both light induced and scotoactive opening, it essentially employs different mechanisms for the rise of pH of the cytoplasm in each of these cases.

Zeiger, Bloom & Hepler (1978) have put forward a chemi-osmotic mechanism. Metabolic reactions in the cell are spatially arranged so as to produce an asymmetrical separation of molecular species across a membrane. This causes a concentration gradient and electro-chemical gradient, thus converting chemical energy to osmotic energy. Proton expulsion leads to an effective electrochemical gradient which the cell can use for work. K^+ salts enter the guard cell, causing turgor change.

Certain chemicals such as fusicoccin (FC) influence stomatal conductance. FC was found to enhance stomatal opening by increasing the H^+ pump

capacity as well as by increasing malate synthesis (Travis & Mansfield, 1979).

STOMATAL OSCILLATIONS

Stomata are rarely in a steady state either in the field or in the laboratory (Raschke, 1975). Oscillations for most plant species have a period between 10 to 50 minutes. An observation by Apel (1966, 1967) showed an oscillation of 2·5 to 4·5 minutes superimposed upon an oscillation with a period of 15 to 30 minutes for maize (see Barrs, 1971). This separation of stomatal cycling into high frequency CO_2-based oscillations and lower frequency water-based oscillations stands up quite well on the whole. Barrs (1971) has summarized the oscillations in stomatal apertures.

Several researchers have modeled the dynamics of stomatal action. Cowan (1972) developed an electrical analog model for the hydropassive feedback loop of stomatal action. Unlike that model, the model developed by Delwiche & Cooke (1977) dealt directly with the plant components. The differential equations which describe their model are based on leaf water fluxes in guard and subsidiary cells. The model predicted hydraulically stable oscillations in the form of a stable limit cycle. Rand *et al.* (1981) analyzed this model and showed the existence of a Hopf bifurcation.

Farquhar & Cowan (1974) have studied the response of stomata to changes in ambient humidity and CO_2 concentration using a control system approach. Cowan (1977) has reviewed stomatal behavior with respect to changes in the environment. He has included dynamic behavior regulated by a hydraulic loop as well as by light and CO_2. This electrical analog model did not show higher frequency oscillations induced by a CO_2 feedback loop. It was concluded that the effect of CO_2 and light level is to influence the hydraulic loop by shifting the phase of the hydraulic oscillations.

The Model

QUALITATIVE DESCRIPTION

We will now describe in words the hypothetical events which we have included in our model of the effects of CO_2 chemistry on stomatal dynamics. Later in this paper we will present a mathematical model based on these effects as well as on previous work which considered only the effects of transpiration (Delwiche & Cooke, 1977).

CO_2 in the ambient atmosphere diffuses into the leaf through the stomatal pores (Fig. 4) and is assimilated into the leaf mesophyll cells. At the same

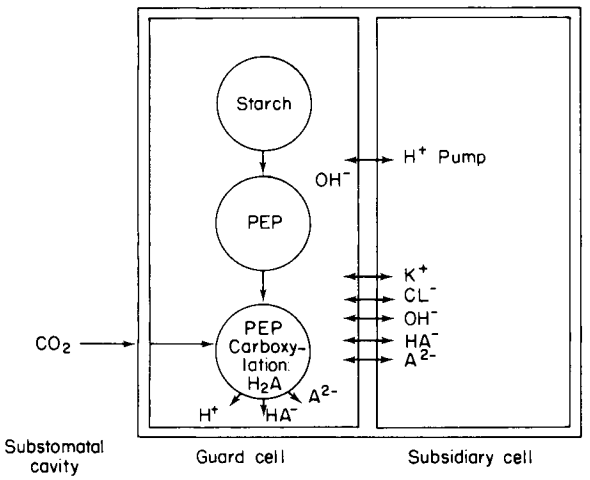

FIG. 4. Schematic diagram of model featuring effects of CO_2 on stomatal dynamics.

time CO_2 is released from inside each mesophyll cell due to respiration. Both of these effects produce a net concentration of CO_2 in the substomatal cavity. Under conditions of high light, CO_2 from respiration most likely contributes little to the CO_2 concentration in the substomatal cavity due to the much greater rate of CO_2 fixation of photosynthesis.

CO_2 is absorbed from the substomatal cavity into the guard cells where it is converted into malic acid (H_2A) by PEP carboxylation. It has been suggested that this chemical reaction provides the CO_2 sensing mechanism responsible for CO_2 feedback (Raschke, 1975).

We assume that when sufficient energy is available due to either light absorption (during the day) or oxidative phosphorylation in mitochondria (during the night) asymmetrical separation of H_2O occurs across the guard cell membrane, i.e., a proton pump is activated (cf. chemiosmotic hypothesis, Zeiger, *et al.*, 1978). This results in the active expulsion of H^+ to subsidiary cells (or to neighboring epidermal cells in plants which do not have subsidiary cells) and in the active expulsion of OH^- to guard cells. The pump generates a pH difference and an electrical potential difference across the membranes separating the guard cell from the subsidiary cell.

Once the H_2A is formed in the cytoplasm of the guard cell, it dissociates into H^+, HA^- and A^{2-} depending on the concentration of H^+, i.e. on the pH of the guard cell cytoplasm (Freiser & Fernando, 1963).

Some of the H^+ ions produced by the dissociation of H_2A combine with OH^- ions to produce water. The rest regulate the pH of the guard cell.

Some of the HA^- and A^{2-} ions may diffuse passively across the cell membranes to the subsidiary cell. The strength of these passive fluxes depends on both the concentration differences and the electrical potential differences between the guard cell and the subsidiary cell.

It has been shown experimentally that K^+ ions move into the guard cell from the subsidiary cell as stomata open (Raschke, 1975). We assume that a passive K^+ flux is set up by the electrical gradient generated by the H^+ pump. In some species OH^-/Cl^- exchange may occur, depending on the availability of Cl^- ions in the subsidiary cell. The electrical charge of the K^+ ions in the guard cell is balanced by that of HA^-, A^{2-} and Cl^- ions.

Finally, the osmotic potential (and thus the water potential) of the guard cell changes in response to the net change in K^+, HA^-, A^{2-} and Cl^- ion concentrations. Water flows passively into the guard cell from the subsidiary cell in response to the change in water potential.

SIMPLIFYING ASSUMPTIONS

We shall make the following assumptions in order to simplify the analysis:

(1) The guard cell pH is assumed to be such that the dissociated malate in the guard cell consists mainly of A^{2-} ions. This assumption is reasonable because guard cell cytoplasmic pH is high compared with the second dissociation constant of malic acid (Raschke, 1979).

(2) For simplicity we assume that no Cl^- ions participate in the ion shuttle. If Cl^- ions are present, they help the A^{2-} ions to balance the charge of the K^+ ions. Since one Cl^- ion balances only one K^+ ion while one A^{2-} ion balances two K^+ ions, the presence of Cl^- increases the osmotica in the guard cell for a given quantity of K^+. However, this effect only complicates the model (by involving an additional differential equation) without providing any fundamentally different phenomenon. See the section on extensions of the model for further discussion.

(3) We assume that the number of K^+ ions in the guard cell at any time is twice the number of A^{2-} ions there. This requires that charge balances occur on a much faster time scale than do membrane fluxes (Hsiao, 1976).

(4) All chemical reactions are assumed to occur on a much faster time scale than membrane fluxes. This permits us to take all chemical reactions to be at quasi-equilibrium.

(5) The total quantity of K^+ ions in the guard cell subsidiary cell complex is assumed to be constant (Raschke, 1979).

(6) The rate of production of malate by PEP carboxylation is assumed to follow Michaelis–Menten kinetics.

(7) The H^+ pump is assumed to actively transport H^+ ions at a rate which is independent of other model parameters.

MATHEMATICAL MODEL OF CO_2 EFFECTS

We begin by writing a form of Ohm's law for the ion flow through the guard cell and subsidiary cell membranes (see Nobel, 1974 p. 120, equation (3.20)):

$$E = FR_{\text{mem}}A_{sg}(J_{H^+} + J_{K^+} - 2J_{A^{2-}}) + E_0 \tag{1}$$

where E = electrical potential difference between the guard cell and the subsidiary cell (volts), E_0 = electrical potential difference due to unbalanced charges, assumed to be zero in this analysis (volts), J_i = flux of species i taken positive when flux direction is from subsidiary cell to guard cell (mole/cm^2 s), A_{sg} = area of interface between guard cell and subsidiary cell (cm^2), R_{mem} = electrical resistance of guard cell and subsidiary cell membranes in series (ohms) and F = the Faraday = 96487 coulombs/mole.

Next we consider the flux terms in equation (1). The H^+ flux is due entirely to the pump, and using assumption (7) may be written as:

$$J_{H^+} = -q \tag{2}$$

where

q = H^+ pump transport rate (mole/cm^2 s).

An expression for the A^{2-} ion flux may be obtained by noting that the net rate of accumulation of A^{2-} ions in the guard cell equals the rate of A^{2-} ion production by carboxylation plus the rate at which A^{2-} ions enter the guard cell from the subsidiary cell. By assumption (3), the rate of accumulation of A^{2-} ions also equals half the rate of accumulation of K^+ ions. This gives:

$$\tfrac{1}{2}A_{sg}J_{K^+} = \frac{V^*HC_{\text{cav}}^{CO_2}}{K^* + HC_{\text{cav}}^{CO_2}} + A_{sg}J_{A^{2-}} \tag{3}$$

where we have used assumption (6), and where $C_{\text{cav}}^{CO_2}$ = CO_2 concentration in the substomatal cavity (mole/cm^3), K^* = Michaelis–Menten constant (mole/cm^3), V^* = maximum enzymatic velocity (mole/s), and H = Henry's law constant. Note that $J_{A^{2-}}$ is negative, indicating flow out of the guard cell.

Here we have used Henry's law, which states that equilibrium at the gas–liquid interface (i.e. at the guard cell wall) requires that the ratio of the concentration of CO_2 in the cell liquid to the concentration of gaseous CO_2 in the substomatal cavity is H. Nobel (1974, p. 330) gives $H = 1{\cdot}19$ at 10°C and $H = 0{\cdot}88$ at 20°C.

Substituting equations (2) and (3) into equation (1) and setting E_0 equal to zero gives:

$$E = FR_{\text{mem}}\left(-qA_{sg} + \frac{2V^*HC_{\text{cav}}^{CO_2}}{K^* + HC_{\text{cav}}^{CO_2}}\right). \tag{4}$$

An expression for the K^+ flux is available in Nobel (1974, p. 110, equation (3.15))

$$J_{K^+} = \frac{pa}{e^a - 1}\left(\frac{N_s}{V_s} - e^a\frac{N_g}{V_g}\right) \tag{5}$$

where

$$a = FE/RT, \tag{6}$$

N_i = mass of K^+ ions in cell i (mole), V_i = volume of cell i (cm^3), p = permeability of guard cell and subsidiary cell membranes in series (cm/s), R = gas constant = 83·141 cm^3 bar/mole K, T = absolute temperature (K), and where subscripts g, s refer to guard cell and subsidiary cell, respectively.

Assumption (5) may be written:

$$N_s + N_g = N_T = \text{constant}. \tag{7}$$

Conservation of mass for K^+ ions gives

$$\dot{N}_g = A_{sg}J_{K^+} \tag{8}$$

Equations (5) to (8) give

$$\dot{N}_g = \frac{paA_{sg}}{e^a - 1}\left(\frac{N_T - N_g}{V_s} - e^a\frac{N_g}{V_g}\right). \tag{9}$$

Since, from equation (6), a depends on E, one must consider equations (9) and (4) simultaneously. These equations represent the effects of CO_2 on stomatal dynamics and will be incorporated into a more comprehensive model in the next section.

MODEL INCLUDING BOTH CO_2 AND HYDRAULIC FEEDBACK LOOPS

We shall append the CO_2-effect equations just derived to a model which has been previously presented (Delwiche & Cooke, 1977) and analyzed (Rand *et al.*, 1980), but which involved only a hydraulic feedback loop. This model may be represented in the functional form (equations (A11) and (A12) in Appendix I):

$$\dot{P}_g = f_1(P_g, P_s, \tilde{\pi}_g) \tag{10}$$

$$\dot{P}_s = f_2(P_g, P_s, \tilde{\pi}_g). \tag{11}$$

Here P_g and P_s are the hydrostatic (turgor) pressure in the guard cell and subsidiary cell, respectively, and $\tilde{\pi}_g$ is the metabolically controlled part of the osmotic pressure in the guard cell. (Note that osmotic potential is the negative of osmotic pressure, see Appendix I, equation (A5).) Delwiche & Cooke (1977) took $\tilde{\pi}_g$ to be a constant and found that the system of equations (10) and (11) nevertheless exhibited a steady state oscillation (a limit cycle in the P_g, P_s plane, Fig. 2).

In order to include CO_2 feedback in this model we will allow $\tilde{\pi}_g$ to vary with time. By assumptions (1), (2), and (3), the only ions responsible for changing $\tilde{\pi}_g$ are K^+ and A^{2-}. Since each A^{2-} ion has two K^+ ions accompanying it in the guard cell (assumption (3)), we may write the Van't Hoff relation (Nobel, 1974, p. 66, equation (2.10)) as:

$$\tilde{\pi}_g(t) = \frac{3}{2}\frac{RT}{V_g}[N_g(t) - N_g(0)]. \tag{12}$$

The variations of $\tilde{\pi}_g$ with time t will therefore be given by equations (9) and (4) which govern $N_g(t)$. However, equation (4) requires that the concentration of CO_2 in the substomatal cavity be known. A recent model (Rand & Cooke, 1980) has provided an equation for $C_{cav}^{CO_2}$ in terms of leaf geometry and biochemistry. The explicit form of this equation is presented in Appendix II, equation (A13), but may be abbreviated by the functional expression:

$$C_{cav}^{CO_2} = f_3(P_g, P_s). \tag{13}$$

(Here $C_{cav}^{CO_2}$ depends on the stomatal diffusion resistance, which depends on the stomatal pore width, which in turn depends on P_g, P_s. See Appendices I, II for details.)

Finally note that the cell volumes V_g, V_s appearing in equations (9) and (12) are not constants, but rather depend linearly upon P_g, P_s, respectively, since the cell walls are assumed to be elastic. See equation (A7) in Appendix I.

In summary, equations (9), (10) and (11) together with auxiliary equations (4) and (13), form a dynamical system of three coupled nonlinear ordinary differential equations which define a flow on the P_g, P_s, N_g state space.

Results and Discussion

In order to study the dynamics exhibited by the above system of ordinary differential equations, numerical integration was performed on a digital computer. Adams' predictor-corrector method was used in conjunction with a Runge Kutta fourth order initialization scheme.

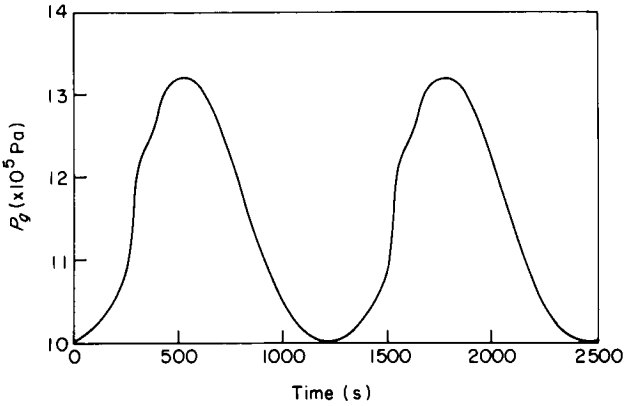

FIG. 5. Hydrostatic (turgor) pressure in the guard cell, P_g, displayed as a function of time for the limit cycle oscillation of Fig. 3.

The parameters chosen for the numerical treatment are listed in Appendix III. For these parameter values the system exhibited a stable limit cycle in P_g, P_s, N_g state space. Figure 3 shows a projection of this limit cycle onto the P_g, P_s plane.

Corresponding to this periodic motion of the system in the P_g, P_s plane, each of the model variables displays a periodic dependence on time. Figures 5–10 show respectively the model's predictions for the time dependence of P_g, P_s, w, $C_{cav}^{CO_2}$, E and N_g.

Consider Fig. 7 which shows pore width w versus time. The large peaks correspond to maximum stomatal opening and are due to the hydropassive

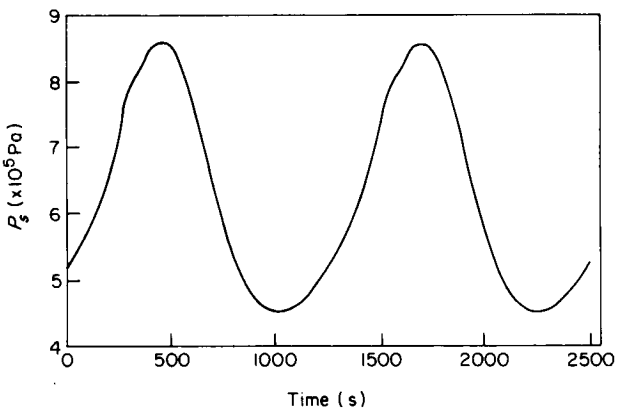

FIG. 6. Hydrostatic (turgor) pressure in the subsidiary cell, P_s, displayed as a function of time for the limit cycle oscillation of Fig. 3.

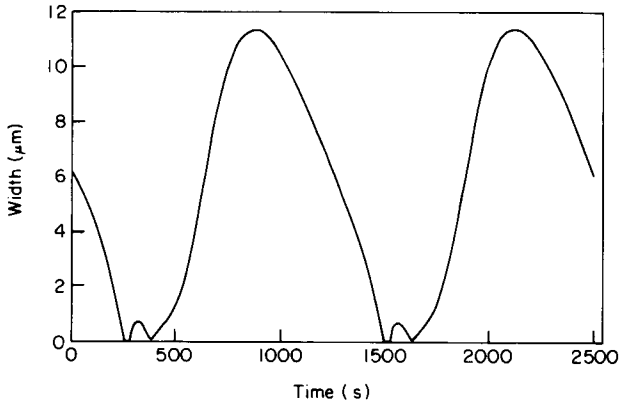

FIG. 7. Pore width, w, displayed as a function of time for the limit cycle oscillation of Fig. 3.

feedback loop. These peaks have a period of about 20 minutes and are essentially the same as those observed by Delwiche & Cooke (1977), see Fig. 2.

However, Fig. 7 also reveals the presence of smaller amplitude oscillations. *These occur when the stomatal pore is nearly closed* and have a period of about 2 minutes. These were not observed by Delwiche & Cooke (1977) and are therefore the result of the CO_2 feedback loop. We believe these oscillations correspond to the high frequency oscillations observed by Apel (1967).

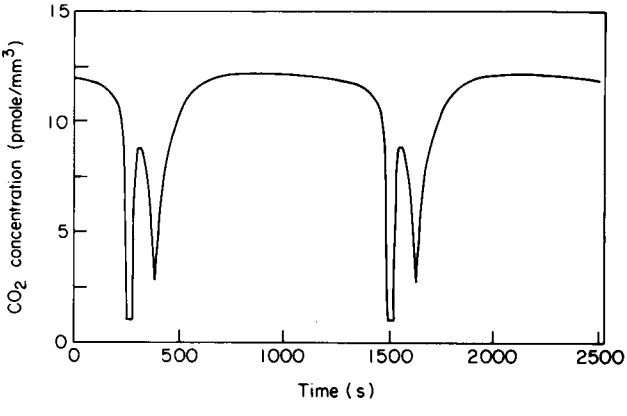

FIG. 8. Concentration of CO_2 in substomatal cavity, $C_{cav}^{CO_2}$ displayed as a function of time for the limit cycle oscillation of Fig. 3.

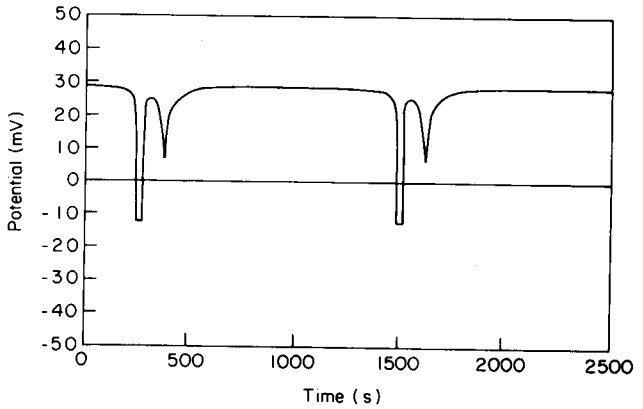

FIG. 9. Electrical potential difference between guard cell and subsidiary cell, E, displayed as a function of time for the limit cycle oscillation of Fig. 3.

In order to verify the presence of the higher frequency oscillation in our stomatal oscillator we consider the model's prediction for the time dependence of N_g (Fig. 10). Figure 11 displays the results of a Fourier analysis of the function $N_g(t)$ shown in Fig. 10. Note the presence of multiple peaks in the spectrum of Fig. 11. In addition to the fundamental period of 20·8 minutes we also see significant contributions at 2·31 minutes and at 1·15 minutes. These latter peaks represent the CO_2 oscillation. The 1·15 minute contribution signifies the presence of a second harmonic component of the basic CO_2 oscillation. The appearance of subharmonics represents typical

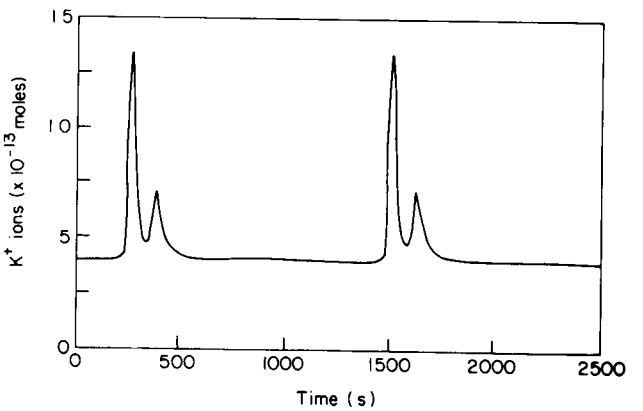

FIG. 10. Mass of K^+ ions in guard cell, N_g, displayed as a function of time for the limit cycle oscillation of Fig. 3.

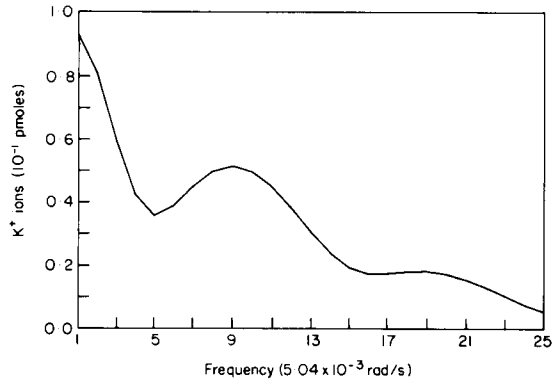

FIG. 11. Fourier analysis of $N_g(t)$ from Fig. 10. The ordinate displays the polar magnitude, $=(A_n^2+B_n^2)^{1/2}$ of the nth Fourier component.

behavior for limit cycles in nonlinear systems (Stoker, 1950, p. 136). In this Fourier analysis we have chosen to study $N_g(t)$ rather than $w(t)$ because the CO_2 feedback loop effects are larger in $N_g(t)$ than in $w(t)$ and hence are easier to demonstrate numerically (cf. Figs 7 and 10).

Note from Figs 8–10 that these oscillations in w occur in synchrony with rapid changes in $C_{cav}^{CO_2}$, E and N_g. As the pore width becomes smaller the concentration of intercellular CO_2 in the stomatal cavity decreases, the voltage in the guard cell drops to a negative value and a large influx of K^+ ions enter the guard cell from the subsidiary cell.

Examination of the numerical solution reveals that w, $C_{cav}^{CO_2}$ and E are all in phase with each other, while N_g leads all of these by about 30 seconds. (Since the behavior is periodic one may also say that N_g lags the others by about 90 seconds.) This may be explained by the *algebraic* relationship between w, $C_{cav}^{CO_2}$, equation (13), and between $C_{cav}^{CO_2}$, E, equation (4), as contrasted with the *differential* equation relating N_g and E, equation (9). An algebraic relationship which does not involve time explicitly requires all related variables to be in phase, while a differential equation like equation (9) has a time constant associated with it related to the observed phase difference between N_g, E. Note also that w is algebraically related to P_g, P_s, equation (A10) in Appendix I, but that P_g, P_s are related by differential equations to N_g, equations (10)–(12).

The short period CO_2 oscillations may be described in words in terms of the mathematical model as follows: An increase in w causes an increase in $C_{cav}^{CO_2}$, which causes an increase in E, equation (4). The greater positive charge of the guard cell relative to the subsidiary cell forces K^+ ions to passively flow out of the guard cell, decreasing N_g, equation (9). Now $\tilde{\pi}_g$

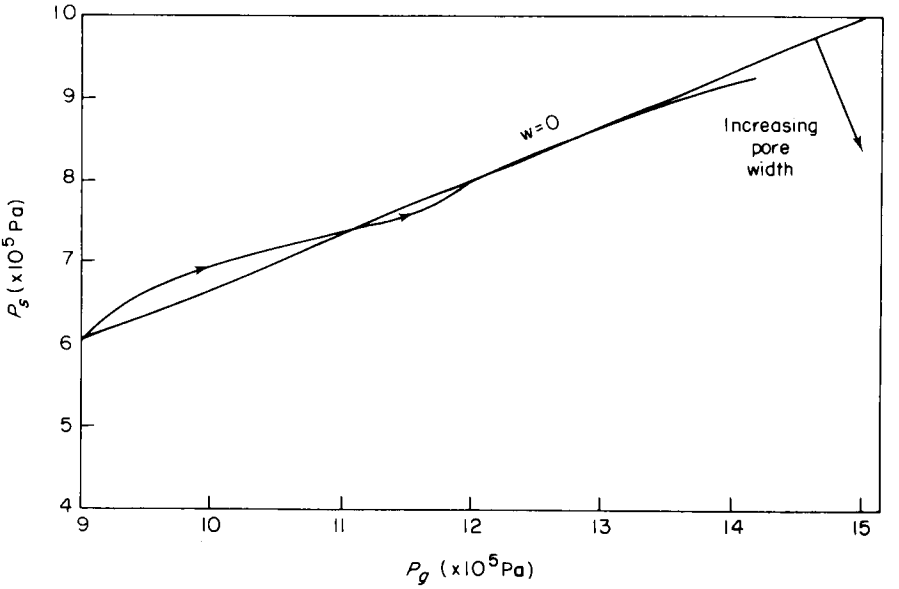

FIG. 12. CO_2 loop oscillation projected onto the P_g, P_s plane exhibited by model described in this paper. Effect of hydropassive loop has been eliminated by equating the concentration of water vapor in the atmosphere outside the leaf to that inside the leaf. Note that this oscillation is not a limit cycle; here the system approaches steady state equilibrium.

decreases, equation (12), causing water to flow out of the guard cell and changing P_g, P_s, equations (10) and (11). This results in a smaller pore width w decreasing $C_{cav}^{CO_2}$, decreasing E, increasing N_g, increasing $\tilde{\pi}_g$ and finally increasing w to complete this cycle.

The CO_2 oscillation may be isolated from the hydropassive oscillation by equating the concentration of water vapor in the atmosphere outside the leaf, C_{ta}^{wv}, to that inside the leaf, C_m^{wv}, (i.e., the atmosphere has 100% relative humidity at leaf temperature). For the other parameters as in URC, but with $C_{ta}^{wv} = C_m^{wv} = 23 \times 10^{-6}$ mm^3/mm^3, we obtained the oscillation shown in Fig. 12.

A comparison of Fig. 12 with Figs 2 and 3 shows that the normal behavior of our model (Fig. 3) may be thought of as a "superposition" of a purely hydropassive oscillation (Fig. 2) and a purely CO_2 oscillation (Fig. 12). Of course, here we are being figurative, since the differential equations of the model are *nonlinear* and therefore strict superposition does not hold.

EFFECTS OF CHANGES IN PARAMETERS

In order to investigate the effects on the CO_2 oscillation of changes in model parameters we suppressed the hydropassive loop by setting $C_{ta}^{wv} =$

C_m^{wv} as in Fig. 12. We considered the influence of the following six parameters on the CO_2 oscillation period and amplitude and on the equilibrium pore width:

(1) membrane permeability to K^+ ions, p in equation (5),
(2) electrical membrane resistance R_{mem} in equation (1),
(3) pump transport rate, q in equation (2),
(4) maximum PEP carboxylation velocity, V^* in equation (3),
(5) Michaelis–Menten constant for PEP carboxylation, K^* in equation (3),
(6) CO_2 concentration in the atmosphere, $C_{ta}^{CO_2}$.

The results of our investigation are summarized in Table 1. Each of the above six parameters was independently changed and the resulting changes in the CO_2 oscillation noted.

TABLE 1

Effect of parameter changes in CO_2 oscillation

	p	R_{mem}	q	V^*	K^*	$C_{ta}^{CO_2}$
Oscillation period	−	−	+	−	+	−
Oscillation amplitude	−	+	+	−	+	−
Equilibrium pore width	none	−	+	−	+	−

(+ = increase, − = decrease)

Some of these effects may be understood by considering the model equations. For example, note that an increase in p causes the magnitude of J_{K^+} to increase, equation (5), and thus causes the rate of K^+ transfer to increase. This decreases the oscillation period.

The effect of q, V^*, K^* and $C_{ta}^{CO_2}$ on equilibrium pore width may be established as follows: Note that increases in q, K^* and decreases in V^* and $C_{ta}^{CO_2}$ all cause the membrane potential E of the guard cell to become more negative, equation (4). At equilibrium, the right-hand side of equation (5) must vanish. Using equation (7), this gives

$$N_g = \frac{N_T}{1+(V_s/V_g)e^a}. \tag{14}$$

From equation (6), a decrease in E causes a to decrease which decreases e^a and which in turn causes an increase in N_g at equilibrium, equation (14). An increase in the osmotic contents of the guard cell causes the pore to open wider as additional water enters the guard cell.

Note also that since p does not appear in the equilibrium equation (14) (see equation (5)), it cannot influence the equilibrium pore width.

COMPARISON WITH EXPERIMENTAL OBSERVATIONS

Most experimental observations of stomatal effects have considered the equilibrium pore width rather than the oscillation itself. For example, the well known result that stomata open wider if the concentration of CO_2 in the atmosphere around the plant is decreased (Meidner & Mansfield, 1968) is in agreement with the model's behavior (Table 1).

Application of abscisic acid (ABA) was found to reduce stomatal aperture (Dubbe, Farquhar & Raschke, 1978). It has been suggested that ABA reduces the electrogenic pump capacity (Raschke, 1977). Our model supports this hypothesis since from Table 1 a decrease in pump capacity q causes a reduction in equilibrium pore width. However, ABA is ineffective at stomatal closure unless CO_2 is present. This suggests that ABA may enhance CO_2 fixation in the guard cell. Our model predicts that an increase in carboxylation rate causes a smaller stomatal aperture since from Table 1 an increase in V^* produces a reduced pore width.

On the other hand, application of fusicoccin (FC) was found to increase the steady state aperture (Travis & Mansfield, 1979). This effect may be due to an increase in the electrogenic pump capacity by FC (Raschke, 1977). Our model supports this hypothesis (Table 1). Moreover, Travis & Mansfield (1979) also found an increase in malate content of the guard cell when FC was applied. In terms of our model, assumption (3) requires that an increase in malate be accompanied by an increase in K^+ ions in the guard cell. From equation (14), at equilibrium N_g will increase if a is decreased and, from equations (4) and (6), this will follow from a decrease in V^*. This leads us to speculate that FC may inhibit CO_2 fixation in the guard cell.

The phenomenon of stomatal opening in the presence of light may be explained by hypothesizing light as an energy source for the electrogenic pump. In the presence of light, the pump capacity q increases causing an increase in pore width (Table 1).

EXTENSIONS OF THE MODEL

In this section we shall consider various ways of extending the model. Consider first the addition of a hydroactive feedback loop to the hydropassive and CO_2 loops already discussed. Hydroactive stomatal closure involves the role of the plant hormone ABA. It has been shown that water

stress produces ABA in leaves (see e.g., Pierce & Raschke, 1980). A hydroactive feedback loop could be included in our model by considering the pump capacity q or the PEP carboxylation velocity V^* to depend on the water potential ψ_m of the leaf mesophyll cells. We have omitted this loop at present due to a lack of information concerning the precise nature of the feedback mechanism.

Consider next the extension of the model which results when the simplifying assumptions (listed above in the description of the model) are relaxed. In this case we would have five differential equations corresponding respectively to mass balance for each of the following ion fluxes: K^+, A^{2-}, HA^-, OH^-, Cl^-. Moreover PEP carboxylation would be described by an additional differential equation. These six differential equations together with the two differential equations (10) and (11) of the hydropassive model (Delwiche & Cooke, 1977) would constitute the extended model. Needless to say the behavior of the resulting system would be considerably more difficult to understand than that of the present model and therefore not justified at this time.

Perhaps the most serious limitation imposed by our simplifying assumptions regards the assumed charge balance between K^+ and A^{2-} ions (assumption (3)). Although this assumption is valid at equilibrium, in general there will be some unbalanced charges in the guard cell. These will change at a rate equal to the net current flow through the membrane. Assumption (3) requires that such unbalanced charges be small, allowing us to neglect the electrical potential generated by the unbalanced charges in the guard cell. Relaxing this assumption would add an additional term to equation (1) for E, which in turn would require an additional differential equation, further complicating the model.

Another important limitation is due to assumption 1, where we assumed that the pH of the guard cell is such that the dissociation of malate produced mainly A^{2-} ions in the guard cell. In fact we expect that the number of A^{2-} ions in the guard cell will be greater than the number of HA^- ions, but that both ions will be present. In relaxing assumption (1) we must append to the model a cubic equation for the pH (Freiser & Fernando, 1963). It seems likely that this will not qualitatively change the model's behavior. Note that our model does not require consideration of the ultimate fate of malate, a question which has not yet been resolved in the literature.

AGRICULTURAL APPLICATION

The influence of $C_{ta}^{CO_2}$ on the equilibrium pore width may have implications for CO_2 enrichment in greenhouses. As $C_{ta}^{CO_2}$ increases, the

equilibrium pore width has been shown to decrease (Table 1). $C_{cav}^{CO_2}$ depends both on the pore width and $C_{ta}^{CO_2}$ (Rand & Cooke, 1980). Therefore, $C_{cav}^{CO_2}$ does not increase in direct proportion to $C_{ta}^{CO_2}$ but depends nonlinearly on $C_{ta}^{CO_2}$. As photosynthesis is a saturation function of $C_{cav}^{CO_2}$, photosynthesis varies in a predictable but complicated manner with $C_{ta}^{CO_2}$.

Moreover, a decreased pore width reduces transpiration rate. Reduced transpiration rate may imply an improved water use efficiency (i.e. number of moles of water vapor evaporated per mole of CO_2 fixed by photosynthesis).

These considerations have been the subject of another study (Upadhyaya, Rand & Cooke, 1981).

Summary and Conclusions

We have proposed a mathematical model of the effects of CO_2 on stomatal dynamics. It consists of a system of three autonomous nonlinear differential equations which were solved numerically.

The model exhibits a stable steady state periodic behavior (a limit cycle) which may be thought of as the superposition of a long (about 20 min.) period hydropassive loop and a short (about 2 min.) period CO_2 loop. These characteristics agree with the experimental work of Apel (1966).

We have investigated the effects of changes in the model parameters on the system's behavior. In particular, the relationship between $C_{ta}^{CO_2}$ and stomatal pore width provides us with a theoretical means of studying the influence of CO_2 enrichment on plant productivity and water use efficiency.

We have proposed a scheme by which a hydroactive feedback loop could be included in the model.

Perhaps the single most important conclusion of this work is the unexpected prediction that the CO_2 loop oscillation occurs only when the stomatal pore is nearly closed.

This research was presented as ASAE Paper No. 80-5517 at the 1980 Winter Meeting of the American Society of Agricultural Engineers at the Palmer House Hotel, Chicago, Illinois, on December 2–5, 1980, and is available from ASAE, St. Joseph, Michigan 49085 in microfiche form.

REFERENCES

APEL, I. P. (1966). *Ber. dt. bot. Ges.* **79,** 279.
APEL, I. P. (1967). *Ber. dt. bot. Ges.* **80,** 3.
BARRS, H. D. (1971). *A. Rev. Pl. Physiol.* **22,** 223.
COOKE, J. R., DEBAERDEMAEKER, J. G., RAND, R. H. & MANG, H. A. (1976). *Trans. ASAE* **19,** 1107.

COOKE, J. R., RAND, R. H., MANG, H. A. & DEBAERDEMAEKER, J. G. (1977). *ASAE paper # 77-5511* St. Joseph, Michigan: American Society for Agricultural Engineering.
COOKE, J. R. & RAND, R. H. (1980). In: *Predicting Photosynthesis in Ecosystem Models* (Hesketh, J. D. & Jones, J. W. eds). Vol. 1. pp. 93–121. Boca Raton, Florida: CRC Press.
COWAN, I. R. (1972). *Planta (Berl)* **106,** 221.
COWAN, I. R. (1977). *Adv. Bot. Res.* **4,** 117.
DELWICHE, M. J. & COOKE, J. R. (1977). *J. theor. Biol.* **69,** 113.
DUBBE, D. R., FARQUHAR, G. D. & RASCHKE, K. (1978). *Pl. Physiol.* **66,** 413.
FARQUHAR, G. D. & COWAN, I. R. (1974). *Pl. Physiol.* **54,** 769.
FREISER, H. & FERNANDO, Q. (1963). *Ionic Equilibria in Analytical Chemistry.* New York: John Wiley and Sons.
HSIAO, T. C. (1976). *Encyclopedia of Plant Physiology.* (Luttge, V. & Pitman, M. G. eds). Vol. 2. pp. 195–221. New York: Springer-Verlag.
LEVITT, J. (1974). *Protoplasm* **82,** 1.
MEIDNER, H. & MANSFIELD, T. A. (1968). *Physiology of Stomata.* New York: McGraw Hill.
NOBEL, P. S. (1974). *Introduction to Biophysical Plant Physiology.* San Francisco: Freeman.
PIERCE, M. & RASCHKE, K. (1980). *Planta.* **148,** 174.
RAND, R. H. & COOKE, J. R. (1980). *Trans. ASAE.* **23,** 601.
RAND, R. H., UPADHYAYA, S. K., COOKE, J. R. & STORTI, D. W. (1980). *J. math. Biol.* **12,** 1.
RASCHKE, K. (1975). *Ann. Rev. Plant Physiol.* **26,** 309.
RASCHKE, K. (1977). In: *Regulation of Cell Membrane Activities in Plants* (Marre, E. & Ciferri, O. eds). Amsterdam: Elsevier/North Holland Biomedical Press.
RASCHKE, K. (1979). *Encyclopedia of Plant Physiology.* (Haupt, W. & Feinleib, M. E. eds). Vol. 7. Heidelberg: Springer-Verlag.
STOKER, J. J. (1950). *Nonlinear Vibrations.* New York: Interscience Publishers.
TRAVIS, A. J. & MANSFIELD, T. A. (1979). *New Phytol.* **83,** 607.
UPADHYAYA, S. K., RAND, R. H. & COOKE, J. R. (1980*a*). *Stomatal Dynamics. Advances in Bioengineering.* (Van C. Mow ed.). pp. 185–188. New York: American Society of Mechanical Engineering.
UPADHYAYA, S. K., RAND, R. H. & COOKE, J. R. (1980*b*). *ASAE Paper 80-5517.* St. Joseph, Michigan: American Society for Agricultural Engineering.
UPADHYAYA, S. K., RAND, R. H. & COOKE, J. R. (1981). *ASAE Paper 81-4017.* St. Joseph, Michigan: American Society for Agricultural Engineering.
ZEIGER, E., BLOOM, A. J. & HEPLER, P. K. (1978). *What's New Pl. Physiol.* **9,** 29.

APPENDIX I

The Hydraulic Loop Model

Since the present model is an extension of the stomatal dynamics model of Delwiche & Cooke (1977), we shall give a brief derivation of the governing equations below.

CONSERVATION OF MASS FOR WATER FLOWING INTO AND OUT OF GUARD AND SUBSIDIARY CELLS

$$\dot{V}_g = J_{sg}A_{sg} \tag{A1}$$

$$\dot{V}_s = J_{ms}A_{ms} - J_{sg}A_{sg} \tag{A2}$$

where V_i = volume of cell i (cm^3), J_{ij} = volume flux of water from cell i to cell j (cm/s), A_{ij} = area of interface between cells i and j (cm^2), and where the subscripts refer to the following types of cells: g = guard cell, s = subsidiary cell, m = mesophyll cell.

THERMODYNAMICS

$$J_{sg} = L(\psi_s - \psi_g) \tag{A3}$$

$$J_{ms} = L(\psi_m - \psi_s) \tag{A4}$$

where ψ_i = water potential in cell i (bar), L = hydraulic conductivity coefficient (cm/bar s).

WATER POTENTIALS

$$\psi_j = P_j - \pi_j - \tilde{\pi}_j, \qquad j = g, s \tag{A5}$$

where P_j = hydrostatic (turgor) pressure in cell j (bar), π_j = osmotic pressure in cell j due to osmotica that remain inside cell j (non-diffusible solutes) (bar) and, $\tilde{\pi}_j$ = osmotic pressure in cell j due to osmotica that are added to or removed from cell j by metabolic processes and diffusion (e.g., CO_2 loop processes) (bar).

In fact we assume $\tilde{\pi}_s = 0$. Delwiche & Cooke (1977) took $\tilde{\pi}_g$ = constant. The present paper replaced this assumption with treatment of $\tilde{\pi}_g$ as an additional state variable (Upadhyaya, Rand & Cooke, 1980*a*, *b*).

CONSERVATION OF SOLUTE MASS

$$\pi_j V_j = \pi_j^0 V_j^0, \qquad j = g, s \tag{A6}$$

where the superscript 0 refers to incipient plasmolysis.

ELASTIC CELLS

$$P_j = \frac{V_j - V_j^0}{V_j^0}\,\varepsilon_j \tag{A7}$$

where ε_j = cell wall elastic modulus for cell j (bar)

CONSERVATION OF MASS FOR TRANSPIRATION STREAM

$$\frac{\psi_r - \psi_m}{R_p} = \frac{c_m^{wv} - c_{ta}^{wv}}{R_t^{wv}} \tag{A8}$$

where ψ_r = water potential at the roots (bar), ψ_m = water potential in the

leaf mesophyll (bar), c_m^{wv} = concentration of water vapor at the mesophyll cell walls (cm^3/cm^3), c_{ta}^{wv} = concentration of water vapor in the turbulent atmosphere adjacent to the leaf surface (cm^3/cm^3), R_p = resistance to flow of water in liquid state between root mesophyll leaf cells (bulk flow) (bar s/cm), R_t^{wv} = resistance to flow of water vapor between mesophyll cells and leaf exterior (diffusion) (s/cm).

DIFFFUSION RESISTANCE

The following expression for R_t^{wv} has become available since the paper by Delwiche & Cooke (1977) was written. It is thought to be more accurate than the expression originally used (Cooke & Rand, 1980, pp. 101, 104).

$$R_t^{wv} = \frac{1}{D^{wv}}\left[l + \frac{2dr^2}{\hat{a}w} + \frac{r^2}{\hat{a}}\ln\left(\frac{8\hat{a}}{w}\right) - r\right] \tag{A9}$$

where D^{wv} = diffusion coefficient of water vapor in air (cm^2/s), l = thickness of still air layer adjacent to leaf (cm), $\hat{a}$ = semimajor axis of elliptical stomatal pore (cm), w = pore width (minor axis of elliptical pore) (cm), d = pore depth (distance from leaf exterior to substomatal cavity) (cm) and r = average distance between adjacent pores on leaf surface (cm).

GUARD CELL ELASTOSTATICS

The following expression for pore width w was obtained by using finite element analysis (Cooke *et al.*, 1976)

$$w = \begin{cases} b_0 + b_g P_g + b_s P_s & \text{if } b_0 + b_g P_g + b_s P_s \geq 0 \\ 0 & \text{if } b_0 + b_g P_g + b_s P_s < 0 \end{cases} \tag{A10}$$

where b_0, b_g and b_s are constants.

GOVERNING EQUATIONS

Substituting equations (A3)–(A8) into equations (A1) and (A2), and assuming small volume changes in equation (A7) gives

$$\dot{P}_g = \frac{\varepsilon_g A_{sg} L}{V_g^0}\left[-\left(1 + \frac{\pi_g^0}{\varepsilon_g}\right)P_g + \left(1 + \frac{\pi_s^0}{\varepsilon_s}\right)P_s + \tilde{\pi}_g + \pi_g^0 - \pi_s^0\right] \tag{A11}$$

$$\dot{P}_s = \frac{\varepsilon_s L}{V_s^0}\left[A_{sg}\left(1 + \frac{\pi_g^0}{\varepsilon_g}\right)P_g - (A_{sg} + A_{ms})\left(1 + \frac{\pi_s^0}{\varepsilon_s}\right)P_s\right.$$

$$\left. - A_{sg}\tilde{\pi}_g - A_{sg}\pi_g^0 + (A_{sg} + A_{ms})\pi_s^0 + A_{ms}\left(\psi_r + \frac{R_p(c_{ta}^{wv} - c_m^{wv})}{R_t^{wv}}\right)\right]. \tag{A12}$$

Equations (A9) and (A10) replace R_t^{wv} in equation (A12) with an expression dependent on P_g, P_s. This relationship provides the feedback that causes the model to oscillate.

APPENDIX II

CO_2 Assimilation Model

We summarize here a comprehensive model of CO_2 assimilation in leaves (Rand & Cooke, 1980), which we use in this paper to predict the CO_2 concentration in the substomatal cavity.

CONSERVATION OF MASS FOR CO_2 FLUX INTO THE LEAF

$$\frac{C_{ta}^{CO_2} - C_{cav}^{CO_2}}{R_t^{CO_2}} = \left(\frac{A^{mes}}{A}\right)\rho\frac{(1-k^3)}{3}\Phi(HC_{cav}^{CO_2}) \tag{A13}$$

The left-hand side of equation (A13) represents the diffusive flux of CO_2 from the leaf exterior into the substomatal cavity. The right-hand side of equation (A13) represents the net CO_2 flux assimilated into the leaf mesophyll cells. The parameters and expressions appearing in (A13) are identified as follows: $C_{cav}^{CO_2}$ = concentration of CO_2 in the substomatal cavity (g/cm^3), $C_{ta}^{CO_2}$ = concentration of CO_2 in the turbulent atmosphere adjacent to the leaf surface (g/cm^3), $R_t^{CO_2}$ = resistance to flow of CO_2 between leaf exterior and substomatal cavity (diffusion) (s/cm), $= \frac{D^{wv}}{D^{CO_2}} R_t^{wv}$, cf. equation (A9).

D^{CO_2} = diffusion coefficient of CO_2 in air (cm^2/s), A^{mes} = surface area of mesophyll cells under leaf area A (cm^2), ρ = radius of typical (assumed spherical) mesophyll cell (cm), k = ratio of vacuole radius to cell radius for typical (spherical) mesophyll cell ($k < 1$), H = Henry's law constant (Rand & Cooke, 1980), Φ = net rate of CO_2 assimilation in mesophyll cell cytoplasm = $\Phi_{chl} - \Phi_{pr} - \Phi_{drk}$, Φ_{chl} = chloroplast carboxylation rate (g/cm^3 s),

$$\Phi_{chl} = \frac{V_c K_0 HC_{cav}^{CO_2}}{K_c K_0 + K_0 HC_{cav}^{CO_2} + K_c Q}$$

Φ_{pr} = photorespiration rate (g/cm^3 s)

$$\Phi_{pr} = \frac{tV_0 K_c Q}{K_c K_0 + K_0 HC_{cav}^{CO_2} + K_c Q}$$

Φ_{drk} = dark respiration rate (g/cm^3 s).

Here Φ_{chl} and Φ_{pr} are assumed to follow Michaelis–Menten kinetics, while Φ_{drk} is taken as a constant (Cooke & Rand, 1980).

K = Michaelis–Menten constant (g/cm^3), V = maximum enzymatic velocity per unit volume ($g/cm^3\,s$), Q = oxygen concentration (g/cm^3), t = fraction of glycolate carbon released in photorespiration and where subscripts c, o refer to CO_2 and oxygen, respectively.

Equation (A13) represents a quadratic equation on $C_{cav}^{CO_2}$. As discussed in Rand & Cooke (1980) only one root is positive (the other is negative and must be rejected as extraneous). In terms of the state variables of our stomatal oscillator, equation (A13) gives $C_{cav}^{CO_2}$ as a function of $R_t^{CO_2}$, and hence as a function of w (equation (A9)), and finally as a function of P_s and P_g (see equation (A10)).

APPENDIX III

Parameter Values

The following list gives the parameter values used for the numerical treatment of the differential equations of the model. They are based on values given in Nobel (1974), Cooke & Rand (1980), Rand & Cooke (1980), Delwiche & Cooke (1977).

Parameter	Value	Equation in which it first appears
$\hat{a}$	10^{-2} mm	A9
A^{mes}/A	30	A13
A_{ms}	$6{\cdot}3\times10^{-3}$ mm^2	A1
A_{sg}	$6{\cdot}3\times10^{-4}$ mm^2	1
b_0	0	A10
b_g	$1{\cdot}4\times10^{-3}$ mm/bar	A10
b_s	$-2{\cdot}1\times10^{-3}$ mm/bar	A10
$C_{ta}^{CO_2}$	$1{\cdot}28\times10^{-11}$ mole/mm^3	A13
C_m^{wv}	23×10^{-6} mm^3/mm^3	A8
C_{ta}^{wv}	$4{\cdot}6\times10^{-6}$ mm^3/mm^3	A8
D^{CO_2}	16 mm^2/s	A13
D^{wv}	26 mm^2/s	A13
d	10^{-2} mm	A9
H	1	3
K^*	2×10^{-12} mole/mm^3	3
K_c	$7{\cdot}5\times10^{-12}$ mole/mm^3	A13

Parameter	Value	Equation in which it first appears
K_0	$Q/K_0 = 0{\cdot}7$	A13
k	0·9	A13
L	10^{-6} mm/bar s	A3
l	100 mm	A9
$N_g(0)$	4×10^{-13} mole	12
N_T	$11{\cdot}6\times10^{-12}$ mole	7
p	$4{\cdot}8\times10^{-4}$ mm/s	5
Q	$Q/K_0 = 0{\cdot}7$	A13
q	11×10^{-10} mole/mm^2 s	2
R_{mem}	6×10^{8} ohm	1
R_P	5×10^{5} bar s/mm	A8
r	0·0674 mm	A9
T	25°C	6
t	0·25	A13
V_g^0	$4{\cdot}2\times10^{-6}$ mm^3	A6
V_s^0	$4{\cdot}2\times10^{-5}$ mm^3	A6
V^*	$6{\cdot}9\times10^{-13}$ mole/s	3
V_c	$V_0/V_c = 0{\cdot}5$	A13
V_0	$V_0/V_c = 0{\cdot}5$	A13
ε_g	50 bar	A7
ε_s	50 bar	A7
π_g^0	22·5 bar	A6
π_s^0	15 bar	A6
ρ	5×10^{-3} mm	A13
ψ_r	−3 bar	A8